Deposition Diseases and 3D Domain Swapping

Review

Melanie J. Bennett,[1] Michael R. Sawaya,[1] and David Eisenberg[1,*]
[1] Howard Hughes Medical Institute
Departments of Chemistry and Biochemistry and
   Biological Chemistry
University of California, Los Angeles
Los Angeles, California 90095

Protein aggregation is a feature of both normal cellular assemblies and pathological protein depositions. Although the limited order of aggregates has often impeded their structural characterization, 3D domain swapping has been implicated in the formation of several protein aggregates. Here, we review known structures displaying 3D domain swapping in the context of amyloid and related fibrils, prion proteins, and macroscopic aggregates, and we discuss the possible involvement of domain swapping in protein deposition diseases.

Introduction

Deposition diseases are characterized by aggregation of proteins encoded by the afflicted individual's own genome. The soluble proteins associated with such diseases often perform well-characterized and essential biological functions under normal circumstances. However, in the disease state, provoked by a change in environment or genetic predisposition, some part of the native fold is lost, thus exposing a template for the growth of aggregates. The importance of this conformational change in triggering aggregation has led to the term conformational disease to describe these disorders.

From the structural biologist's point of view, it is helpful to divide deposition diseases into two broad categories distinguished by whether or not the deposited aggregates have the properties of amyloid fibrils. Amyloid fibrils are typically composed of two or more protofilaments, each with a central spine of β strands running perpendicular to the fibril axis (cross-β spine), as evidenced by the ability of fibrils to orient the dye Congo red (producing birefringence under polarized light) and by the appearance of a cross-β diffraction pattern. Extracellular deposition of these fibrils is found in ~25 well-defined clinical syndromes called amyloidoses, each associated with a characteristic protein or peptide that constitutes the fibril (Pepys, 2006; Sipe and Cohen, 2000; Westermark et al., 2005) (green circle in Figure 1). Several amyloid diseases, such as Alzheimer's and type II diabetes, are associated with the deposition of amyloid fibrils but have not been proven to be caused by such deposits (Pepys, 2006).

Other diseases differ from the amyloidoses in that the associated fibrils are intracellular (e.g., huntingtin, α-synuclein), and, in some cases, fibrils are not associated with human disease (e.g., Sup35 fibrils associated with the [PSI+] phenotype in yeast). Such fibrils are referred to as "amyloid-like." Also, in many laboratories, researchers infer the structure of amyloid by studying amyloid-like fibrils that can be formed from a variety of proteins in vitro. Thus, amyloid-like fibrils differ from classical amyloid in that they are not extracellular, disease-associated deposits. Nevertheless, at a fundamental level, amyloid-like fibrils share many of the same biophysical characteristics of amyloid fibrils, for example, the presence of cross-β spines.

The second category of deposition disorders includes "nonamyloid" fibrils or aggregates, which lack cross-β spines. In sickle cell anemia (Hemoglobin S [HbS]; pink circle in Figure 1) and the serpinopathies (α1-antitrypsin and neuroserpin; orange circle), the nonamyloid fibrils that are formed retain native structures. In other diseases, the nonamyloid fibrils and aggregates have yet to be characterized in detail (blue box in Figure 1). A deepened understanding of the underlying mechanisms of protein aggregation is crucial for the development of diagnostics and therapeutics for deposition diseases, which are so devastating to affected individuals and so costly to society. Here, we consider 3D domain swapping as a mechanism for forming some of the fibrils and aggregates that occur in deposition diseases.

Mechanisms for Forming Protein Fibrils and Other Deposits

In general, what are the mechanisms that account for the specific self-association of proteins? Structural data so far suggest that there are three possible mechanisms: cross-β spine, end-to-end stacking, and 3D domain swapping. Figure 1 shows a Venn diagram that classifies a number of proteins involved in deposition diseases, cellular assemblies, or in vitro aggregates according to their mechanisms of association. As shown by the proteins in overlapping areas, in some cases more than one mechanism may be operative. We consider these mechanisms separately as follows.

The cross-β spine mechanism of association has historically been inferred from the cross-β diffraction pattern observed for most classical, disease-associated amyloid fibrils and a number of amyloid-like fibrils that occur in vitro (green circle in Figure 1). Amyloid and amyloid-like fibrils appear in electron microscopy as rigid, nonbranching ultrastructures that are of varying length, are ~60–130 Å in diameter, bind Congo red, and display "apple-green" birefringence under polarized light (Sipe and Cohen, 2000; Westermark et al., 2005). Amyloid-like fibrils can be formed in vitro from a variety of proteins with all classes of secondary structure (e.g., RNase A Q_{10} mutant [Sambashivan et al., 2005] or myoglobin [Fandrich et al., 2003]). It has been suggested that virtually any protein can form amyloid-like fibrils under appropriate conditions (Chiti et al., 1999). Despite the diversity of structures in the native state, in the fibrillar state the proteins convert at least partially to stacked β sheets with main chain hydrogen bonds parallel to the fibril axis and side chains perpendicular to the fibril axis, as inferred from the ~4.7 Å meridional and 10 Å

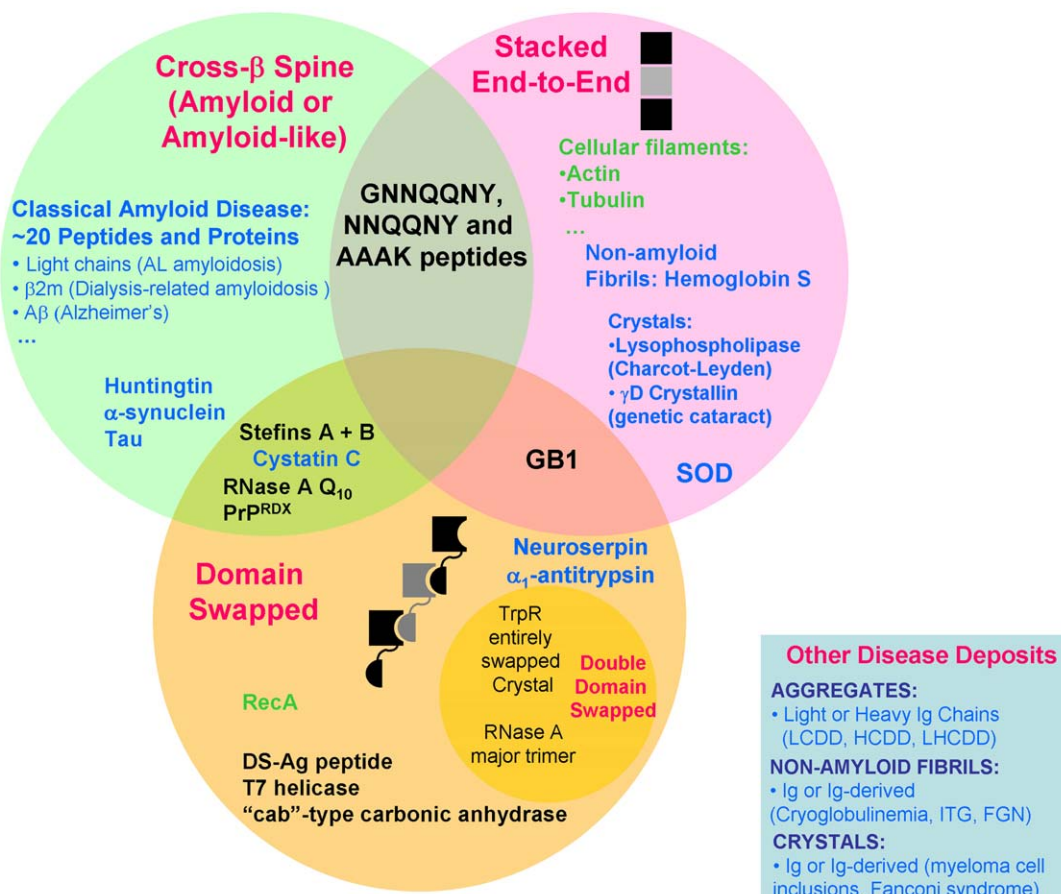*Correspondence: david@mbi.ucla.edu

Figure 1. Higher-Order Protein Assemblies in Health and Disease

A Venn diagram showing the structural mechanisms by which proteins form filaments, fibrils, or aggregates in cellular assemblies, human diseases, and model systems in vitro. Proteins that form amyloid or amyloid-like fibrils, as defined by the presence of a cross-β spine (Sunde et al., 1997), are shown in the green circle. Amyloid fibrils are those that (1) are associated with disease, (2) are extracellular in localization, and (3) display Congo red binding and birefringence (Pepys, 2006; Sipe and Cohen, 2000; Westermark et al., 2005). Some amyloid fibrils have been suggested to form by pathways involving 3D domain swapping (e.g., cystatin C [Nilsson et al., 2004; Sanders et al., 2004] and β2-microglobulin [Eakin et al., 2004]). Fibrils formed from some proteins, such as SOD, are believed to involve stacking of subunits that contain native-like β sheets (Elam et al., 2003). Some amyloid-like fibrils have an intracellular localization or differ from amyloid in tinctorial properties (e.g., in Huntington's or Parkinson's disease). Other amyloid-like fibrils include those that are not associated with deposition diseases in vivo, such as fibrils derived from model protein or peptide systems in vitro (e.g., myoglobin [Fandrich et al., 2003], RNase A Q_{10} [Sambashivan et al., 2005], PRP[RDX] [Lee and Eisenberg, 2003], GNNQQNY [Nelson et al., 2005], and AAAK [actual sequence KFFEAAAKKFFE] peptides [Makin et al., 2005]). Other proteins not associated with deposition disease include the cytoskeletal proteins actin (Holmes et al., 1990) and tubulin (Downing and Nogales, 1999), shown in the pink circle, as well as GB1 (Louis et al., 2005), RecA (Story et al., 1992; Xing and Bell, 2004), DS-Ag (Ogihara et al., 2001), T7 helicase (Sawaya et al., 1999), "cab"-type carbonic anhydrase (Strop et al., 2001), and the trpR entirely domain-swapped crystal (Lawson et al., 2004). The blue box lists some examples of disease deposits for which there is insufficient structural information for classification into the Venn diagram. Note that some disease-associated fibrils lack a cross-β spine (e.g., Hemoglobin S [Dykes et al., 1978; Wishner et al., 1975]; serpins, reviewed in [Lomas and Carrell, 2002]; and nonamyloid fibrils identified histopathologically [negative Congo red binding assays; blue box]).

equatorial reflections in fiber diffraction (Blake and Serpell, 1996; Sunde et al., 1997).

Details of the cross-β spine have recently been revealed by atomic resolution single-crystal X-ray diffraction studies of the peptide GNNQQNY from the prion-determining domain of Sup35 (Nelson et al., 2005). The structure shows that the cross-β spine is comprised of a pair of β sheets and reveals that strands within each sheet interact through conventional backbone hydrogen bonds as well as hydrogen bonds between glutamine and asparagine side chains. Two sheets interact through a "steric zipper" in which dehydrated side chains are tightly enmeshed (Nelson et al., 2005). Thus, the steric zipper is the molecular interaction that binds the two sheets in a cross-β spine. The cross-β spine is a form of self-complementation that can be combined with domain swapping (e.g., hinge loop of RNase A Q_{10} [Sambashivan et al., 2005]). Inasmuch as one considers a "minimal" cross-β motif to exist (i.e., a pair of zipped strands), the cross-β spine in peptide structures can

be said to involve end-to-end stacking as well (e.g., GNNQQNY and other peptides [Makin et al., 2005; Nelson et al., 2005]).

Native proteins that stack like building blocks but do not form cross-β spines are familiar examples of aggregation through end-to-end stacks (pink circle) (e.g., HbS or cytoskeletal proteins). The lack of a cross-β spine does not preclude involvement in serious disease: sickle cell anemia involves fibrils of HbS that impair red blood cell function. Fibrils of HbS resemble amyloid fibrils (although they are somewhat larger, at 210 Å diameter), and they display optical birefringence of a bound chromophore (heme) (reminiscent of the birefringence of Congo red bound to amyloid fibrils) and provide evidence that native-like aggregated structures can yield highly ordered fibrils in deposition diseases. This supports the idea that native-like structures can be involved in disease fibril formation, which would also occur in 3D domain swapping. Other proteins involved in normal cellular processes (e.g., cellular assemblies in pink circle in Figure 1) also form higher-order structures by end-to-end stacks.

Stacking of proteins in an end-to-end manner has been suggested to produce a cross-β diffraction pattern if it occurs in a protein containing native β sheets. Transthyretin (TTR) (Correia et al., 2006; Serag et al., 2002), superoxide dismutase (SOD) (Elam et al., 2003), cystatin C (Janowski et al., 2005), and GB1 (Louis et al., 2005) form fibrils that have been suggested to contain native-like structures comprised of β sheets or β sandwiches. Though such structures would not contain cross-β spines, a cross-β diffraction pattern could result if β strands were fortuitously oriented perpendicular to the fiber axis.

3D Domain Swapping: Beyond Small Oligomers

3D domain swapping is a third mechanism for aggregation of proteins, and it is the mechanism that we shall focus on in this review. Domain swapping is a mechanism for forming homodimers and higher-order oligomers by the exchange of protein domains. The "swapped" domain can be an element of secondary structure or a globular protein domain, and it is linked to the "core" of the protein by a "hinge loop" (Figure 2A). In the simplest example, homodimerization, domain swapping takes place when a pair of "closed monomers" (Figure 2A) opens to form a pair of "open monomers" by rotating about the hinge loop. Domains are then exchanged between protomers, reconstituting two "functional units" (FU), each comprised of residues from two protein chains. The preservation of the FU in domain-swapped dimers was first elegantly elucidated in complementation studies of inactivated RNase A molecules, which reconstitute activity after domain swapping (Crestfield et al., 1962). Such a swap is referred to as being closed ended, because the swap is reciprocal; there are no unsatisfied (exposed) domains (as in the dimer schematic shown in Figure 2A, bottom right). However, open-ended "runaway" domain swaps, in which domain-swapped oligomers propagate (as a protofilament) with at least one unsatisfied domain at each terminus (as in the filament shown in Figure 2A, top right), also occur.

There are two features of domain swapping that implicate it as a mechanism for linking protomers into oligomers, aggregates, or fibrils such as those involved in deposition diseases (Figure 2A). First, domain swapping is compatible with a diverse set of proteins such as those involved in deposition diseases. It does not require a specific sequence since the formation of this type of intermolecular interface is primarily a matter of self-complementation. That is, the domain-swapped dimer or higher oligomer is stabilized by the same interdomain interactions that are found in the closed monomer (red in Figure 2A). Only the hinge loop changes significantly in conformation upon domain swapping. Many examples of domain swapping have been observed by crystallography and NMR. These include more than 30 closed-ended small oligomers, but also a few open-ended runaway swaps (Liu and Eisenberg, 2002). Human prion protein (Figure 2B) and cystatin C (Figure 2C) are two examples of proteins that are domain swapped and are also known to be involved in amyloid or prion disease (Janowski et al., 2001; Knaus et al., 2001; Prusiner, 1998). The hinge loops form a small β sheet in each.

The second feature of domain swapping that implicates it in deposition diseases is the strength of the bond that it forms between protomers. Amyloid deposits are characteristically resistant to proteolysis. This tight enmeshing of proteins might partially explain how the proteins are able to evade the cell's protein degradation machinery. Domain swapping creates a strong, flexible tether. In effect, the entire intramolecular interface in the monomeric protein forms an intermolecular contact in the oligomer. The result is the production of unusually large interfaces due to numerous protein-protein interactions that evolved in the closed monomer.

Several biochemical studies have implicated domain swapping in the formation of fibrils from proteins involved in conformational diseases, such as hamster prion protein PrP^{RDX} (Lee and Eisenberg, 2003), cystatin C (Jaskolski, 2001; Nilsson et al., 2004; Sanders et al., 2004), and β2-microglobulin (Eakin et al., 2004). The DS-Ag designer peptide also forms fibrils by domain swapping. DS-Ag fibrils retain their native α-helical structure within fibrils (Ogihara et al., 2001) and provide an example of domain swapping in a nonamyloid fibril.

Structural studies have also uncovered potential roles for domain swapping in the architecture of oligomers, fibers, and other aggregates. The structures reviewed here demonstrate that domain swapping can lead to higher-order aggregates in diverse ways, some of which may be relevant both for cellular assemblies and deposition diseases.

Evidence for Runaway Swaps: Infinite Linear Filaments in Crystal Structures

Infinite linear filaments have been observed in several crystals, lending support for the open-ended runaway swap model (Figure 2A). Such structures provide a means of observing filamentous assemblies that would otherwise be intractable by single-crystal diffraction or NMR methods. In these structures, domain exchange occurs between molecules related by screw-axis symmetry within crystals. These include T7 helicase (Figure 3A) (Sawaya et al., 1999) and RecA (Story et al., 1992; Xing and Bell, 2004), which have 6_1 screw axes, and also include α1-antitrypsin (Huntington et al., 1999) (Figure 3B) and "cab"-type carbonic anhydrase (Strop et al., 2001), which have 2_1 screw axes. Two of these
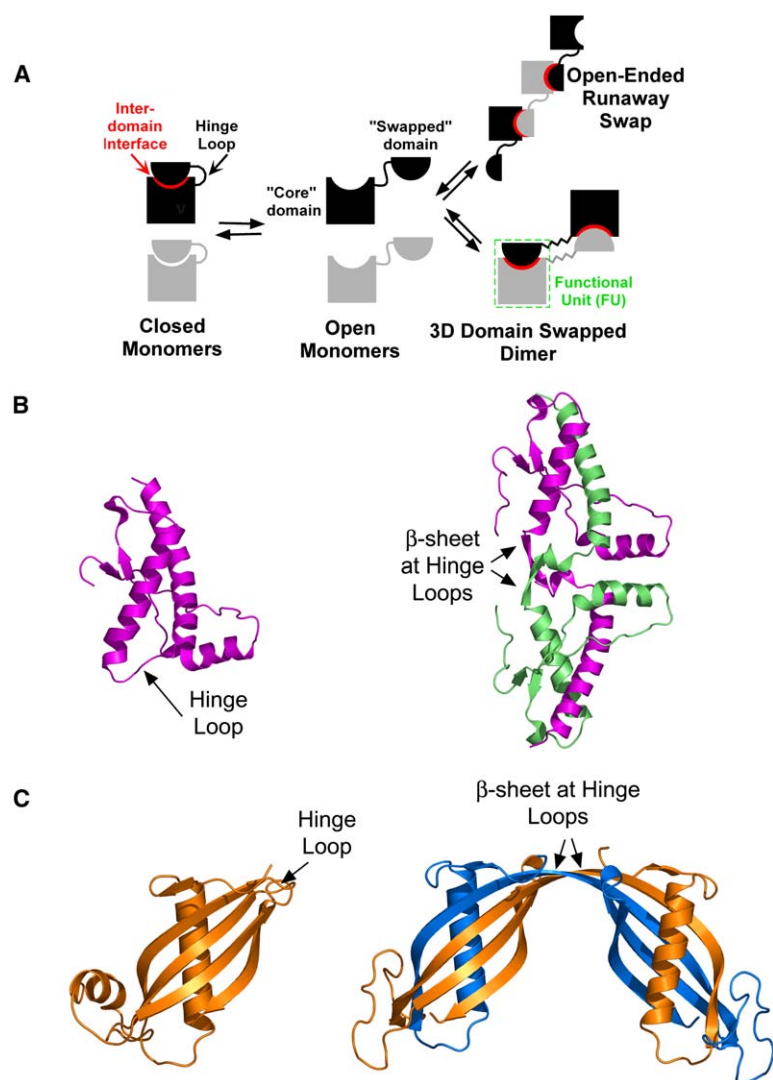
Figure 2. Introduction to 3D Domain Swapping and Examples of Closed Homodimers in Amyloid and Prion Proteins

(A) Structures involved in 3D domain swapping. A closed monomer is a single protein chain folded into two (or more) domains (square or semicircle) with an interdomain interface between them (red). Domains are connected by a flexible hinge loop. Open monomers formed by mutation or changes in environmental conditions can be converted to domain-swapped dimers or higher oligomers. In the domain-swapped structures, the interdomain interface is reformed. Domain swapping can be "closed-ended," with all domains satisfied (as in the dimer), or "open-ended," with unsatisfied domains. The functional unit (FU) is shown in the green dashed box and is comprised of domains from different polypeptide chains. In this example, the FU is essentially identical to the structure of the closed monomer, with the exception of the hinge loop. The hinge loop is the only segment of the structure that changes conformation significantly upon 3D domain swapping.

(B) Monomeric (Zahn et al., 2000) and dimeric (Knaus et al., 2001) human prion protein (PrP^C; residues 90–231). The hinge loops in dimeric PrP^C form a small antiparallel β sheet with six main chain hydrogen bonds, as well as a short helix.

(C) Monomeric chicken cystatin (Bode et al., 1988) and dimeric human cystatin C (Janowski et al., 2001). The hinge loops in dimeric cystatin form an antiparallel β sheet. Mutants of cystatin C form amyloid deposits in a hereditary hemorrhagic stroke disorder. Ribbon diagrams were made with PyMOL (DeLano, 2006).

proteins are also known to form polymers in solution (RecA and α1-antitrypsin). Domain-swapped filaments of the type illustrated by these examples would not include the cross-β spines required for amyloid or amyloid-like fibrils. However, as shown by the example of HbS, a cross-β spine is not essential for producing large fibers that may be involved in disease. In addition, domain swapping can be combined with a cross-β spine as seen in RNase A (discussed below).

To qualify as domain swaps, the interface in the open-ended oligomer must be identical to the interface in the closed reference molecule. This and the following paragraph show how four crystalline arrays qualify as runaway domain swaps. We consider T7 helicase and α1-antitrypsin filaments to be quasi domain swaps, because each has a structurally characterized "closed" counterpart that is very close in sequence to the protein that forms the open-ended filament. The closed counterpart of the 4E fragment of T7 helicase is the 4D fragment hexamer, which differs by having a 30 residue N-terminal extension (Figure 3A, left), and the closed counterpart of the Pittsburgh variant of α1-antitrypsin (M358R) is the S variant closed monomer (E264V) (Figure 3B, left).

Note that the closed reference state can include closed oligomers in addition to closed monomers, as depicted in Figure 2A. In each of the filaments in Figure 3 (right panel), the intersubunit interface that binds the filament together is an interface that is also present in the closed reference molecule.

The other examples of domain-swapped filaments, those formed by *M. thermoautotrophicum* "cab"-type carbonic anhydrase and *E. coli* RecA, are likely to be bona fide swaps, although the closed reference states of the identical proteins have not been structurally characterized at atomic resolution. In solution, *M. thermoautotrophicum* "cab"-type carbonic anhydrase is a tetramer that is expected to be similar to dimers and octomers of β-type carbonic anhydrases from other organisms (Strop et al., 2001; Suarez Covarrubias et al., 2005). In addition to the filaments that have been widely studied, *E. coli* RecA forms a closed ring, which is presumably similar to that characterized in a different organism by electron microscopy (Yu and Egelman, 1997).

The example of the T7 helicase 4E fragment from *E. coli* (Figure 3A) illustrates the general features of an open-ended runaway swap. The assembly of the T7
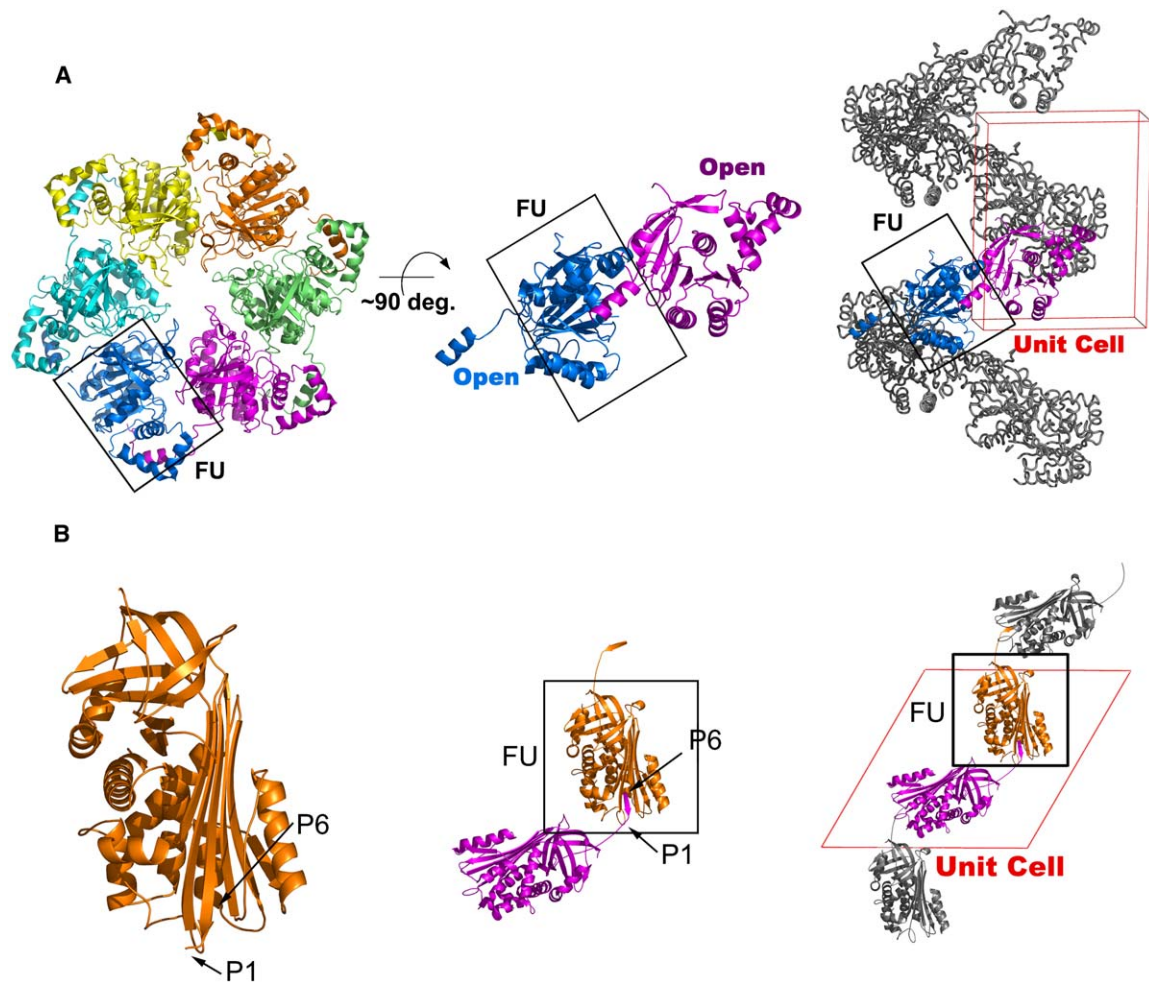
Figure 3. Domain-Swapped Filaments in Crystals

Infinite linear filaments are formed in which each subunit is related to the next by a crystallographic screw-axis (a 2_1 axis for α1-antitrypsin; a 6_1 axis for T7 helicase). Each subunit (a covalent polypeptide chain in T7 helicase, and a cleaved polypeptide chain in α1-antitrypsin) is identified by a unique color. The closed monomer or small oligomer (e.g., hexamer for T7 helicase) is shown on the left. The open dimer is defined as a structure containing a single FU (indicated by a black box) and open ends that can potentially interact with other subunits (middle). In the infinite linear filament (right), the open dimer is highlighted in colored ribbons and the unit cell is indicated as a red box.

(A) The T7 helicase 4D fragment (residues 241–566) is an intertwined hexamer (left) (Singleton et al., 2000). The FU highlighted in the figure corresponds to a hypothetical closed monomer. The T7 helicase 4E fragment (residues 272–566) can be described as an open dimer that contains a single FU (middle) (Sawaya et al., 1999). The view of the open dimer (middle) is rotated by $\sim$90° about the horizontal axis relative to the closed hexamer (left). Within the crystal, the T7 helicase 4E fragment forms a crystal-wide helical filament (right). 6_1 symmetry-related subunits along a single axis are shown. Neighboring filaments related by unit translations are not shown.

(B) α_1-antitrypsin cleaved at the P1-P1$'$ reactive center peptide bond is a monomer (FU) with the P14-P3 segment inserted into β sheet A (Engh et al., 1989; Loebermann et al., 1984). During crystallization of a naturally occurring Pittsburgh mutant (M358R) of α_1-antitrypsin, the P7-P6 peptide bond is cleaved. A complete FU is formed in the open dimer in which residues P6-P3 form a β strand that is swapped. The addition of subsequent subunits results in a domain-swapped filament within the crystal (Huntington et al., 1999). Other proteins that form infinite filaments by domain swapping include "cab"-type carbonic anhydrase (Strop et al., 2001), DSAg designer peptide (Ogihara et al., 2001), and RecA (Story et al., 1992; Xing and Bell, 2004).

helicase filament (Figure 3A, right) can be described as a 1D assembly, like beads on a string, in which subunits are related by screw symmetry, forming a helical structure. Each FU is formed by the interactions between two swapped domains: the "core" domain and an N-terminal helical "swapped" domain (Figure 3A, middle). Addition of monomers to this open dimer forms a "runaway"-swapped filament in the crystal (Figure 3A, right). A related construct, called the 4D fragment, which has an additional 30 residues at its N terminus, forms a closed hexamer with 6 FUs (Figure 3A, left). The 4E filament is

stabilized by the same interdomain interactions as in the closed 4D hexamer.

Similarly, α1-antitrypsin forms filaments structurally related to its closed counterpart. α1-antitrypsin is part of the serpin family, and its function involves cleavage and insertion of the reactive center loop into a β sheet (Lomas and Carrell, 2002). The cleaved S variant α1-antitrypsin closed monomer (Figure 3B, left) forms after a proteolysis event at P1-P1$'$ in the reactive center loop. The filament in Figure 3B (right panel) is formed from the Pittsburgh variant (M358R) of α1-antitrypsin,

which is cleaved at P7-P6 during crystallization and cannot form a closed monomer (Figure 3B, middle). Thus, the swap is irreversible. This is reminiscent of proteins such as staphylococcal nuclease, which irreversibly converts from a closed monomer to a swapped dimer after a hinge loop deletion (Green et al., 1995).

The extensive crystal contacts between subunits in these runaway domain swaps are comparable to those that stabilize biological homodimers or biologically relevant filamentous structures (Table 1). In general, 3D domain swapping produces unusually large intersubunit interfaces due to numerous protein-protein interactions that evolved in the closed monomer (e.g., RNase A single swap homodimers). Several groups have found that the assembly states of proteins in solution (as end-to-end homodimers) can be inferred from their extensive contact areas in crystals. Ponstingl et al. (2000) found that 85% of proteins could be properly assigned as monomers or dimers solely on the basis of the buried area in crystal contacts. The threshold cutoff used for assigning dimers was 1712 A^2 (total interface area; i.e., 856 A^2 per subunit) (Ponstingl et al., 2000) (Table 1). Each internal subunit in a filament has two such interfaces, with the n−1 subunit and the n+1 subunit, which leads to the relatively high overall values for subunits within filaments.

These large intersubunit interfaces do not, however, imply that domain-swapped filaments will be thermodynamically stable. This is because domain swapping has the special feature that the same intersubunit interface is present in both the filament and the monomer (or small oligomer), which is not true in systems in which subunits associate end-to-end. The interface would, however, stabilize the filament relative to the intermediate open monomer state, which subunits would necessarily have to pass through in order to dissociate the filament. That is, the large interfaces in a domain-swapped filament would be expected to kinetically trap the subunits once assembled.

Thermodynamic stability would instead be affected by other factors, including entropic considerations; additional interfaces formed in the filament (the "open" interface [Bennett et al., 1995]); different conformations of hinge loops (reviewed in Rousseau et al., 2003); structural strains specifically in either the open-ended or closed form, often in regions near the hinge loops (Dehouck et al., 2003); and, potentially, by mutations that favor one or the other form (e.g., hinge loop deletion that prevents a closed monomer from forming). Thus, in some cases, domain-swapped filaments may be the thermodynamically favored form. In other cases, they may be metastable and long lived (as in some domain-swapped oligomers such as the diphtheria toxin dimer [Bennett et al., 1994]).

In general, how do structures observed in crystals relate to those found in vivo? A relationship between crystalline and solution states is established in the literature on biologically relevant filamentous proteins. For example, in HbS, the 2_1 filament observed in crystals (Wishner et al., 1975) is believed to be a fundamental component of the fibers associated with sickle cell anemia (Dykes et al., 1978). Protein filaments have also been observed in crystals of other proteins that form filaments in vivo (e.g., Rad51 [Conway et al., 2004], RecA [Story et al., 1992; Xing and Bell, 2004]).

Table 1. Domain-Swapped Assemblies Captured in Crystals Have Extensive Interfaces Comparable to Those in Biological Assemblies

Protein	Size of Interface per Subunit ($Å^2$)
End-to-End Stacks	
Threshold for biological homodimers (Ponstingl et al., 2000)	>856
End-to-end protofilaments[a]	
Hemoglobin S	2022
Tubulin	2447
3D Domain Swaps	
Single swap homodimers[b]	
RNase A N-terminal swap	1992
RNase A C-terminal swap	1835
Single swap filaments[a]	
T7 helicase	1826
α1-antitrypsin	1775
Double swap aggregate[c]	
TrpR	3500

[a] The only crystal contacts considered here are those that produce a protofilament. Further lateral associations in crystals or biological assemblies are not considered. The area given is the total solvent-accessible surface area buried per subunit upon going from a monomer (open monomer in the case of domain-swapped associations) to an internal molecule (as opposed to a terminal molecule) in a filament. Such an internal molecule has at least two interface contact regions, one with each of the flanking molecules (HbS has four contact regions: with two axial and two lateral neighboring molecules). In the case of tubulin, the internal molecule considered is a β-tubulin monomer flanked by two α-tubulin monomers. Areas were calculated by using MSMS (Sanner et al., 1996) or CCP4 (CCP4, 1994) and did not include water molecules or ligands in the calculations. For each contact region, the area buried was divided by two (to obtain the average area buried per subunit per contact region); these areas were summed over the total number of contact regions to obtain the total area buried per subunit in the protofilament. Coordinates used were: 2HBS (Hemoglobin S), 1Z2B (tubulin), 1CR0 (T7 helicase), and 1QMB (α1-antitrypsin).
[b] The area buried per subunit in going from an open monomer to a swapped homodimer. Coordinates used were: 1F0V (C-terminal swap) and 1A2W (N-terminal swap).
[c] Area buried in going from an open dimer to a swapped molecule in the crystalline array, based on an area of 875 $Å^2$/subunit buried between a single E/F helix domain and the core domain. There are four such contacts per open dimer in the crystal. Coordinates used: 1MI7 (trpR).

Further evidence that domain-swapped filaments can exist in vivo comes from the serpin family of proteins, which are involved in human disease. As we have discussed above and in Figure 3B, the P6-P7-cleaved Pittsburgh variant of α1-antitrypsin undergoes irreversible domain swapping within the crystals. Polymers of cleaved α1-antitrypsin have also been characterized in solution by biochemical and ultrastructural techniques, demonstrating that similar filaments occur in solution (Mast et al., 1992). In disease states, uncleaved neuroserpin and α1-antitrypsin polymerize by a "loop-sheet" mechanism (reviewed in Lomas and Carrell, 2002), which involves a domain-swapping event that is similar, but not identical, to that shown in Figure 3B.

The number of structures of crystallized filaments is relatively small, and smaller still is the subset of such filaments with features of domain swapping. However, taken together, the examples of infinite linear filaments
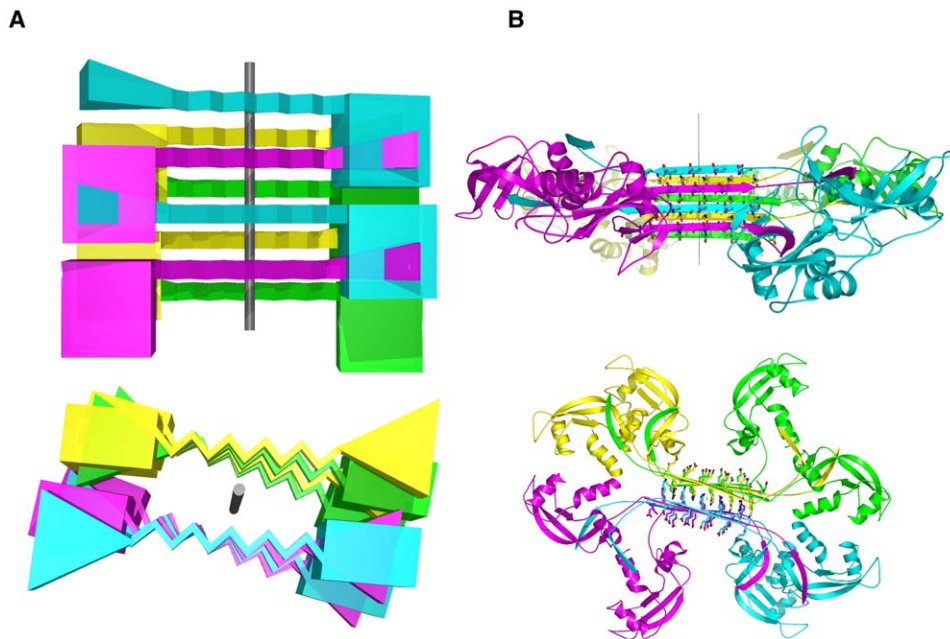
Figure 4. RNase A Q_{10} Amyloid-like Fibrils Combine Domain Swapping with a Cross-β Spine

(A) Schematics of an open-ended runaway domain swap with a cross-β spine formed by glutamines at the hinge loop (upper panel, side view; lower panel, top view). Each core domain of RNase A is shown as a cube, and the C-terminal β strand is shown as a triangle. Molecules 1–4 (blue and magenta) comprise a runaway domain swap with a β sheet formed by their hinge loops (shown as pleated strips). Molecules 5–8 (green and yellow) form a similar runaway swap and β sheet. The 2_1 axis is shown in gray.

(B) Proposed model for an RNase A Q_{10} fibril (upper panel, side view; lower panel, top view; Sambashivan et al., 2005). Packing of side chains between the two sheets forms the cross-β spine. Specifically, the glutamines in the hinge loops (shown in ball-and-stick) act as a steric zipper that binds the two sheets together.

in crystals illustrate some of the energetic and mechanistic properties that may generally characterize filaments formed by open-ended runaway 3D domain swapping.

Domain Swapping with a Cross-β Spine

3D domain swapping has also been studied in fibrils of a model protein, bovine pancreatic RNase A, by biochemical and ultrastructural techniques (Sambashivan et al., 2005). RNase A provides a favorable model system for verification of domain swapping in amyloid-like fibrils in vitro by use of inactive mutants that can reconstitute activity only when domain swapping occurs. Under certain conditions, wild-type RNase A undergoes domain swapping to dimers and trimers whose structures have been determined by X-ray crystallography (Liu et al., 1998, 2001, 2002). Wild-type RNase A does not form fibrils and is not associated with a deposition disease. However, a mutant form with a polyglutamine insertion in its hinge loop (RNase A Q_{10}) forms amyloid-like fibrils in vitro. These fibrils are both domain swapped and possess a cross-β spine, as assessed by a combination of Congo red assays, fiber diffraction, enzyme activity assays, and electron microscopy (Sambashivan et al., 2005).

Molecular modeling provides a theoretical structure that can account for the structural and biochemical properties of the RNase A Q_{10} fibrils (Figure 4). In this model, the hinge loops between swapped domains in RNase A Q_{10} are β strands that form two β sheets, which then associate into a cross-β spine, while peripheral domains undergo domain swapping (Sambashivan et al., 2005) (Figure 4). Specifically, monomers 1–4 (colored blue

and magenta) form an open-ended runaway swapped filament (similar to those described in the previous section) in which the C-terminal β strand of monomer 1 swaps into the core domain of monomer 2, the C-terminal β strand of monomer 2 swaps into the core domain of monomer 3, and so on. The hinge loops form a central β sheet that packs against an identical β sheet formed by the other half of the protofilament (monomers 5–8; colored green and yellow). Thus, the hinge loops form the cross-β spine, while the peripheral domains are stabilized by runaway domain swapping.

Double Domain Swapping: Different Assemblies of the Same Protein

In addition to single domain swapping, described in the sections above, recent structural results have suggested the existence of a phenomenon we term *double domain swapping*, which is defined as the simultaneous exchange of two structural elements. Double domain swapping provides increased diversity and flexibility in the types of structures that can be formed from a single protein, including branched aggregates, which are not possible with single domain swapping. Such branched aggregates could account for some nonfibrillar disease deposits or in vitro aggregates.

The original description of domain swapping assumed that only a single domain per protein would swap (Bennett et al., 1995). However, recent studies on bovine RNase A have revealed that a single protein can swap more than one domain. The oligomerization of RNase A has been studied for over 40 years, and it forms domain-swapped oligomers upon lyophilization from
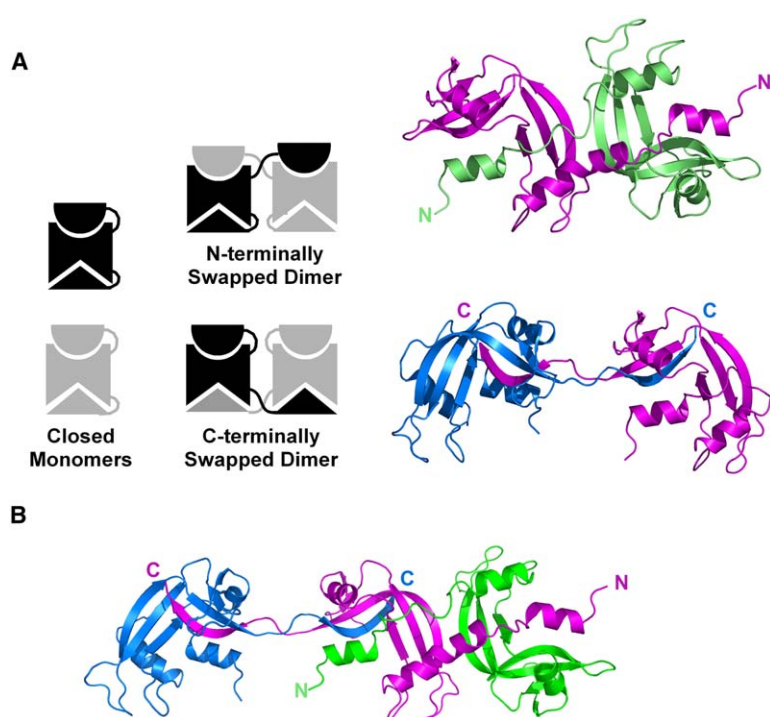
Figure 5. A Single Protein Can Swap More Than One Domain: The Example of RNase A

(A) A generic protein can be described as having two terminal domains (N or C terminus) and a core domain (left). Single domain swapping of the N terminus leads to a closed dimer, as in the crystal structure of the RNase A minor dimer (Liu et al., 1998) (top). Single domain swapping of the C terminus leads to a different closed dimer, as in the crystal structure of the RNase A major dimer (Liu et al., 2001) (bottom). The magenta subunit is shown in the same orientation in both the major and minor RNase A dimer structures. (B) Both domains can be swapped simultaneously in RNase A (double domain swapping). Proposed model for the double domain swapped major trimer that has been characterized biochemically (Liu et al., 2002).

acetic acid (Crestfield et al., 1962) or other conditions, including increased temperature and concentration (reviewed in Libonati and Gotte, 2004). Crystallographic and biochemical studies have dissected the structures of dimers (Liu et al., 1998, 2001), trimers (Liu et al., 2002), and tetramers (Gotte and Libonati, 2004) that form by domain swapping. These studies have shown that RNase A is a special example of domain swapping: it has two "swappable domains."

Crystallographic results demonstrate that RNase A forms two types of closed dimers that swap either the N- or C-terminal segment (Liu et al., 1998, 2001) (Figure 5A). Swapping of the N- or C-terminal domains in RNase A can be controlled by varying the unfolding conditions. Harsher conditions that lead to greater unfolding favor the C-terminal swap in simulations and experiments (Esposito and Daggett, 2005; Gotte et al., 2003).

The "major trimer" of RNase A has been characterized biochemically and forms a double domain-swapped structure in which both N- and C-terminal domains are exchanged (Liu et al., 2002) (Figure 5B). Theoretical models have been proposed for tetrameric, pentameric, and hexameric conformers (Gotte et al., 2006; Libonati and Gotte, 2004) that are believed to similarly involve double domain swapping.

Double domain swapping has novel features compared to single domain swapping (Figure 6A), including the potential for avidity and branched morphology. We define the Swapping Capacity (SC) of a protein as the total number of partner domains that are required to form complete FUs from all of its domains.

That is, SC provides an upper limit on the number of molecules with which a protein of N swappable domains may interact:
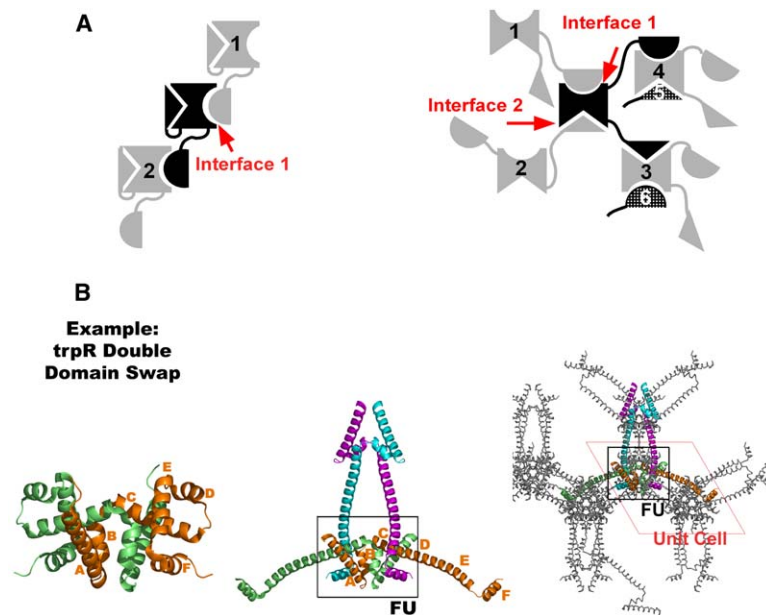
$$SC = \text{Swapping Capacity} = N^2 + N. \qquad (1)$$

A protein with one swapped domain has the potential to interact with only two additional neighboring domains before two complete FUs are formed; therefore, the protein can only produce a 1D linear arrangement (Figure 6A, left), which may be open ended or cyclic. In contrast, a protein with two swappable domains has the potential to interact with up to six other molecules to "satisfy" its domains in complete FUs; therefore, the protein has the potential to form either linear or branched structures (Figure 6A, right).

Due to the self-complementary nature of domain swapping, the SC does not, however, predict the number of molecules with which a given monomer actually interacts. For example, RNase A has two swappable domains and hence an SC of six. However, in the double swapped structure of the RNase A major trimer, each monomer binds only one or two other molecules (Figure 5B). In theoretical structures for RNase A pentamers and hexamers, each monomer binds up to three other molecules (Gotte et al., 2006). In contrast, in the double swapped *E. coli* trp repressor (trpR) structure (discussed below), each dimer interacts with six other dimers, the maximum predicted by the SC.

Thus, double domain swapping provides a mechanism for forming different assemblies of the same protein. Proteins can form both linear filaments and branched aggregates by swapping different domains. The many oligomeric forms of RNase A provide evidence of this. For example, the cyclic RNase A minor trimer can be considered to be a linear filament that has circularized to satisfy all of its domains (Liu et al., 2002) (not shown), whereas the RNase A major trimer is a branched assembly that has also satisfied all of its domains (Figure 5B).

Aside from expanding the available morphologies of assembly, another feature of double domain swapping is that it opens the possibility for multiple binding

Figure 6. Double Domain Swapping Can Lead to Branched Aggregates

(A) Single and double domain-swapped structures have different properties. Open-ended structures formed by single domain swapping must always be linear filaments or cyclic structures, in which each monomer can bind, at most, two additional molecules (left). Double domain swapping can lead to linear or branched aggregates (right). In double domain swapping, each molecule can form four interfaces involving up to six other molecules, leading to potential avidity effects.

(B) Double domain swapping occurs in trpR crystallized in aqueous alcohol (Lawson et al., 2004). The crystal is formed by bona fide double domain swapping between obligate dimeric subunits (Schevitz et al., 1985). The boxed FU in the figure corresponds to this closed-ended dimer. Upon crystallization in aqueous alcohol, the E/F helix domains are loosened from the core domain and swapped with other molecules (Lawson et al., 2004) (middle and right). Helices E and F of the magenta and cyan chains form the same intermolecular bonds as helices E and F of the orange and green chains, respectively, in the closed-ended dimer. Within the crystal, trpR forms an infinite branched aggregate (right). Symmetry-related subunits within a 35 Å radius are shown in gray, and the chains forming a single domain-swapped FU are colored.

interfaces between a single protein monomer and other subunits that are in a covalently or noncovalently tethered array. This could lead to avidity effects that stabilize aggregates (see "Domain Swapping and Avidity").

Proteins in general may be capable of swapping more than one domain. There are now more than 40 examples of domain-swapped oligomers in which the swapped domain is often just an element of secondary structure, such as a β strand or an α helix (Liu and Eisenberg, 2002). Thus, even single-domain proteins can be thought of as consisting of a "core" domain and two "swappable" terminal domains. RNase A, which first revealed this phenomenon, is arguably the best-studied domain-swapping protein. As more structures are determined under different conditions, double domain swapping may be observed in other proteins. Runaway double domain swapping may account for some aggregates.

Domain Swapping and Avidity

Avidity can result when "receptors" A and B are connected by a linker, resulting in a new molecule, AB, whose binding affinity for a ligand is given by:

$$K_{AB} = c\,(K_A * K_B), \qquad (2)$$

where K_A and K_B are the individual affinity (association) constants, and c is a correction factor that accounts for the receptors' linkage, which can be favorable or unfavorable (Jencks, 1981; Mammen et al., 1998). In practice, linking receptors is often favorable ("the avidity effect"), as in tight binding of multivalent Ig receptors to cell-surface ligands or the observation of higher affinities in covalent reagents as compared to substituent components (Shuker et al., 1996). An important feature in avidity is that both of the receptors must be tethered to one another and that their ligands must be tethered to one another, either noncovalently (e.g., by insertion of two receptors into the same cell surface) or covalently (e.g., by disulfide bonds or peptide bonds). The binding of tethered receptors to their tethered ligands can be thought of as increasing the apparent strength of binding because both receptors must release from their ligands simultaneously for complete dissociation to result. Alternatively, from the viewpoint of association, avidity can be thought of as resulting from the increased effective concentration of the second moiety (receptor B) once the first moiety (receptor A) is bound.

In domain swapping, the concept of avidity can be applied by considering the binding of individual domains rather than that of whole proteins. Thus, an open monomer with one swappable domain (Figure 2A, middle) can be viewed as a bivalent, covalently tethered reagent in which a semicircle "receptor" and "square" receptor are linked by the hinge loop. The release of only one "receptor" (e.g., the gray semicircle domain) will not result in dissociation of the homodimer shown in Figure 2A (lower right).

In an aggregate of the type pictured in Figure 6A (right panel), avidity will also result. The central black molecule is connected to its own black domains through covalent peptide bonds. It binds the aggregate through multiple noncovalent interdomain interactions. Each of the surrounding gray molecules is similarly tethered within the aggregate through noncovalent and covalent bonds (not shown in Figure 6A, right, for clarity). Thus, the release of the single black semicircle domain from its contact with molecule 4 will not release the central black molecule from the aggregate. Instead, it remains bound by virtue of its interactions with molecules 1, 2, and 3. Also, the release of a single domain will not, in general, break the aggregate into two smaller aggregates. In contrast, the open-ended filament pictured in Figure 6A (left panel) can be broken in two by releasing only a single black domain, because molecules 1 and 2 are not tethered to one another.

We also note that single domain swapping can result in avid interactions in cases where molecules are tethered to one another (for example, in cases where molecules are inserted at cell surfaces, as in domain swapping between Ig domains in cadherins [Chen et al., 2005] or hemolin [Su et al., 1998]).

trpR: An Entirely Domain-Swapped Crystalline Array
The structure of trpR determined in aqueous alcohol provides insight into the types of aggregated structures that can be formed by double domain swapping. Under these conditions, trpR forms an entirely domain-swapped, crystal-wide array (Figure 6B) (Lawson et al., 2004). That is, the crystal itself is a very large, supramolecular assembly held together by domain swapping.

The crystal is formed by bona fide double domain swapping between obligate dimeric subunits, which undergo open-ended swapping of their E/F helix domains (the green and orange E/F helices in Figure 6B, middle). Within the crystals, each dimer satisfies its domains by interacting with six other dimers, the maximum predicted by the SC. Each trpR dimer is itself a pseudo domain-swapped protein that has a highly intertwined structure but no monomeric homolog (Figure 6B, left). The FU in the double-swapped crystal consists of one of these dimers, which has a core domain (helices A, B, and C of two polypeptide chains) and two swappable domains (helices E/F of each chain). In the presence of aqueous alcohol during crystallization, the swappable E/F helix domains are loosened from their core domains, and a crystalline assembly occurs (Figure 6B, right) in which each protein dimer binds others by domain swapping. In this process, the D helix region also changes in conformation, acting as a hinge loop.

Each dimer in the crystal interacts with a total of six other dimers to form complete FUs from all of its domains. If we focus on the orange/green dimer (Figure 6B, middle), we see that its core domain (helices A, B, and C from both chains) binds the E/F helices of the magenta molecule (first dimer partner) and the E/F helices of the cyan molecule (second dimer partner) to form a complete FU (boxed in black). The green E/F helices require a core domain (third dimer partner; not shown) and another E/F helix domain (fourth dimer partner; not shown) to make another complete FU. Similarly, the orange E/F helices require a core domain and another E/F helix domain to make the final complete FU (fifth and sixth dimer partners; not shown).

The swapping of trpR dimers also occurs in aqueous alcohol solution (Lawson et al., 2004). It has been suggested that hydrophobic interactions in the closed dimer are disrupted under the crystallization conditions used, and, indeed, domain swapping has also been observed in other proteins in aqueous alcohol, including cyanovirin (Yang et al., 1999), cyclophilin 40 (Taylor et al., 2001), and RNase A (Gotte et al., 2003).

The entirely swapped trpR crystal structure demonstrates that double domain swapping can lead to extended branched aggregates. Similar aggregates could conceivably account for some nonamyloid disease deposits, or deposits in vitro, although these would not typically be crystalline, as in the trpR case.

Closed-Ended Domain-Swapped Oligomers as Building Blocks
Closed-ended 3D domain swapping can also lead to higher-order assemblies within crystals. That is, domain-swapped dimers can stack in an end-to-end manner to form higher-order interactions. This was previously noted in CD2, in which a deletion mutant forms a domain-swapped dimer that generates tetramers within the crystal with an interface of 2000 A^2 (Murray et al., 1998). At least two recent structures have noted a combination of closed-ended domain swapping and end-to-end stacking in β-rich assemblies.

End-to-end stacking of swapped homodimers in a β-rich assembly is illustrated by the structure of N-terminally truncated llama VHH-R9 domain (Spinelli et al., 2004). In the domain-swapped homodimer, the swapped domain is the C-terminal strand of an Ig fold, and a new β sheet of 7 residues is formed at the hinge loop (Figure 7A). The hinge loop β sheet interacts with edge β strands from neighboring Ig folds in the crystal, forming an infinite β structure throughout the crystal (Spinelli et al., 2004).

In a recent structure of cystatin C, domain-swapped dimers associate into a crystal-wide assembly (Janowski et al., 2005). The hinge loop in the cystatin C dimer is flexed relative to other cystatin C structures (compare Figures 2C and 7B), bringing the β sheets within the dimer into a parallel position. Two dimers interact to make a tetramer (Figure 7B), and packing of the tetramers within the crystal produces an array extending in three dimensions in which β sheets are all perpendicular to a common axis. A single continuous filament from this array is highlighted in Figure 7C (right panel). Thus, the structure is partially consistent with a cross-β diffraction pattern, although the intermolecular sheet-sheet packing expected to produce a 10 Å equatorial reflection is lacking. Cystatin C also associates into tetramers and octamers in other crystal forms (Janowski et al., 2004), in part by interactions involving the hinge loop β sheets. It is not clear as yet how these different assemblies may be related to disease processes. A stacked filament structure with aligned β sheets has also been proposed to account for the amyloid-like fibrils formed from GB1 domain-swapped dimers (Louis et al., 2005).

Implications for Conformational Disease
How relevant are domain-swapped filaments, aggregates, and closed-ended homodimers to conformational disease? There are now a few biochemical and biophysical studies that implicate domain swapping in amyloidosis (e.g., cystatin C [Jaskolski, 2001; Nilsson et al., 2004; Sanders et al., 2004] and β2-microglobulin [Eakin et al., 2004]). However, the only direct structural evidence we have is the observation of closed-ended domain-swapped homodimers of human PrP and cystatin C in various crystal structures (Figures 2B, 2C, and 7B). Such structures, if they exist in vivo, may undergo further end-to-end stacking and assembly, as suggested for cystatin C (Janowski et al., 2004, 2005; Sanders et al., 2004) (e.g., Figure 7C), thus acting as building blocks in either fibril assembly, or perhaps in the formation of "dead-end" products. A different model has been proposed for hamster PrP^{RDX}, in which a runaway open-ended domain swap forms a cross-β spine
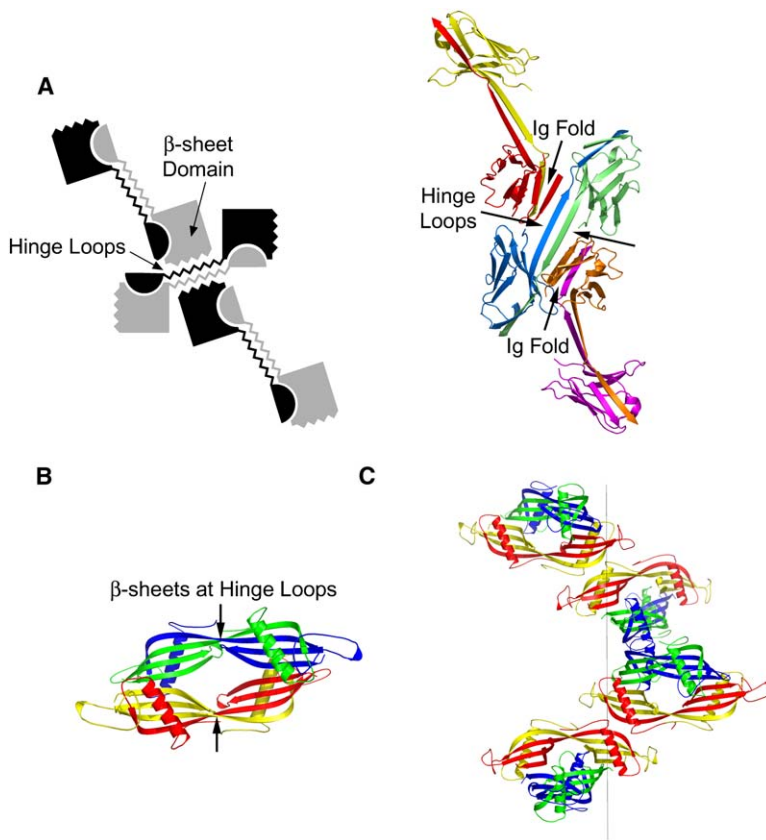
Figure 7. Closed-Ended Domain Swapping Can Lead to Higher-Order Aggregates

(A) Llama VHH-R9 domain forms a crystal-wide β sheet structure by interactions with the hinge loops (Spinelli et al., 2004).

(B) Cystatin C forms a supramolecular structure within one crystal form, in which β sheets are oriented perpendicular to a common axis (Janowski et al., 2005). Two cystatin C swapped dimers form a tetramer.

(C) Tetramers form β-rich filaments. Here, a single continuous filament is highlighted.

by interaction of hinge loops (Lee and Eisenberg, 2003), similar to the proposed model for RNase A (Figure 4). It remains to be determined how, if at all, 3D domain swapping is involved in fibrillization of these proteins in vivo. We have reviewed here the available structural information on higher-order assemblies involving domain swapping, which demonstrate some ways that filamentous or aggregated structures can be formed, some of which share features with amyloid or other deposition disease deposits.

Several structures reveal that 3D domain swapping can produce novel β strands, which are characteristic of amyloid fibrils. New β sheets are formed at hinge loops in PrP (Figure 2B), cystatin C (Figures 2C, 7B, and 7C), and llama VHH-R9 domain (Figure 7A). In the latter two proteins, the β sheets at hinge loops mediate higher-order interactions in crystals (Figure 7A and [Janowski et al., 2004; Spinelli et al., 2004]). The proposed model for the RNase A fibril also includes a new β sheet formed by the hinge loops, which creates the cross-β spine at the core of the protofilament (Figure 4). To the extent that they are involved in forming higher-order structures, novel hinge loop β strands can be considered a type of cryptic epitope (not present in the normally folded monomer) associated with increased aggregation or fibrillization.

The conversion of hinge loops to β structures can also relieve structural "frustration," which has been proposed to be associated with amyloid fibril formation from some proteins (Kallberg et al., 2001). Several amyloidogenic proteins contain "frustrated" or "discordant" regions in the monomers, where residues do not adopt the most favored, predicted β strand conformations, but instead form helices (Kallberg et al., 2001). In PrP, the region in and near the hinge loop in the dimer (Knaus et al., 2001) is such a frustrated region, and the structural discordance is relieved in the domain-swapped dimer by the β strand conformation of the hinge loop (reviewed in Thirumalai et al., 2003).

Other domain-swapped structures are open-ended filaments, albeit without amyloid cross-β spines (Figure 3). Nonamyloid fibrils, both swapped and nonswapped, are known to be involved in some conformational diseases. These include HbS fibrils in sickle cell anemia, nonamyloid fibrils in some immune cell proliferative diseases, neuroserpin fibrils involved in encephalopathy, and α1-antitrypsin fibrils manifesting in systemic disorders such as cirrhosis and emphysema. Neuroserpin and α1-antitrypsin are members of the serpin family that polymerize via a "loop-sheet" mechanism (reviewed in Lomas and Carrell, 2002), which involves a domain-swapping event that is similar, but not identical, to that shown in Figure 3B. Open-ended swapping may also be combined with a cross-β spine to form amyloid or amyloid-like fibrils (as in the example of RNase A Q_{10}, Figure 4).

How might one determine if 3D domain swapping were involved in fibrils of globular proteins? An essential feature would be that fibrils would retain elements of the native structure that could be probed by biophysical techniques, ligand binding, activity assays, or antibody binding. For example, DSAg fibrils possess their native α-helical structure as assessed by FTIR (Ogihara et al., 2001), and RNase A fibrils reconstitute native activity from inactive mutants by domain swapping

(Sambashivan et al., 2005). Domain-swapped fibrils could also retain native disulfide bonds, as previously suggested for hamster PrP^{RDX} (Lee and Eisenberg, 2003). A lack of activity, native disulfides, or native ligand binding, however, does not prove a lack of domain swapping. It is possible that these properties could be disrupted during domain swapping if they involve residues located in the hinge loop, which changes conformation upon swapping.

Domain swapping is consistent with some characteristic aspects of conformational diseases. Like other mechanisms for self-complementation, including the cross-β spine (Nelson et al., 2005), domain swapping can account for species barriers and sequence specificity in prions, because aggregates are held together by sequence-specific interactions. The ability to form long-lived metastable species by domain swapping could explain how two stable conformations (closed monomer and fibril) can exist for the same globular protein without violating Anfinsen's principle (proteins fold spontaneously to their native states). We note that recent studies on suc1 mutants revealed that a metastable monomer is the initial species formed upon folding at micromolar concentrations, even when the domain-swapped dimer is favored thermodynamically (K$_d$ = nanomolar) (Rousseau et al., 2004). Could some deposition disease proteins be metastable monomers that slowly interconvert to thermodynamically stable swapped fibrils?

Finally, domain swapping could provide a rationale for the formation of both fibrils and aggregates from an identical protein in some deposition diseases, if such deposits retain native-like structures. The formation of different types of deposits from the same protein can occur in some lymphoproliferative disorders in which light chains are overproduced, leading to AL (amyloidosis of light chains; amyloid fibrils) and LCDD (light chain deposition disease; amorphous aggregates) (Kaplan et al., 1997; Stokes et al., 1997).

The diversity of domain-swapped structures continues to increase: from small oligomers to "infinite" filaments and an entirely domain-swapped crystal. There are now a number of structures that show that domain swapping is a common mechanism for conformational switching in dimers and trimers (Liu and Eisenberg, 2002). The domain-swapped aggregates captured in crystals that we have reviewed here suggest that domain swapping may be a mechanism for forming more elaborate, larger assemblies. When these structures occur in a regulated way, they may be involved in some biologically relevant cellular assemblies, such as those formed by cell-surface binding proteins (e.g., hemolin [Su et al., 1998] and cadherin [Chen et al., 2005]). Alternatively, unregulated domain swapping may be involved in the formation of aggregates in vitro or in some deposition diseases.

References

Bennett, M.J., Choe, S., and Eisenberg, D. (1994). Domain swapping: entangling alliances between proteins. Proc. Natl. Acad. Sci. USA 91, 3127–3131.

Bennett, M.J., Schlunegger, M.P., and Eisenberg, D. (1995). 3D domain swapping: a mechanism for oligomer assembly. Protein Sci. 4, 2455–2468.

Blake, C., and Serpell, L. (1996). Synchrotron X-ray studies suggest that the core of the transthyretin amyloid fibril is a continuous β-sheet helix. Structure 4, 989–998.

Bode, W., Engh, R., Musil, D., Thiele, U., Huber, R., Karshikov, A., Brzin, J., Kos, J., and Turk, V. (1988). The 2.0 Å X-ray crystal structure of chicken egg white cystatin and its possible mode of interaction with cysteine proteinases. EMBO J. 7, 2593–2599.

CCP4 (Collaborative Computational Project, Number 4) (1994). The CCP4 suite: programs for protein crystallography. Acta Crystallogr. D Biol. Crystallogr. 50, 760–763.

Chen, C.P., Posy, S., Ben-Shaul, A., Shapiro, L., and Honig, B.H. (2005). Specificity of cell-cell adhesion by classical cadherins: Critical role for low-affinity dimerization through β-strand swapping. Proc. Natl. Acad. Sci. USA 102, 8531–8536.

Chiti, F., Webster, P., Taddei, N., Clark, A., Stefani, M., Ramponi, G., and Dobson, C.M. (1999). Designing conditions for in vitro formation of amyloid protofilaments and fibrils. Proc. Natl. Acad. Sci. USA 96, 3590–3594.

Conway, A.B., Lynch, T.W., Zhang, Y., Fortin, G.S., Fung, C.W., Symington, L.S., and Rice, P.A. (2004). Crystal structure of a Rad51 filament. Nat. Struct. Mol. Biol. 11, 791–796.

Correia, B.E., Loureiro-Ferreira, N., Rodrigues, J.R., and Brito, R.M. (2006). A structural model of an amyloid protofilament of transthyretin. Protein Sci. 15, 28–32.

Crestfield, A.M., Stein, W.H., and Moore, S. (1962). On the aggregation of bovine pancreatic ribonuclease. Arch. Biochem. Biophys. S1, 217–222.

Dehouck, Y., Biot, C., Gilis, D., Kwasigroch, J.M., and Rooman, M. (2003). Sequence-structure signals of 3D domain swapping in proteins. J. Mol. Biol. 330, 1215–1225.

DeLano, W.L. (2006). The PyMOL Molecular Graphics System (http://www.pymol.org).

Downing, K.H., and Nogales, E. (1999). Crystallographic structure of tubulin: implications for dynamics and drug binding. Cell Struct. Funct. 24, 269–275.

Dykes, G., Crepeau, R.H., and Edelstein, S.J. (1978). Three-dimensional reconstruction of the fibres of sickle cell haemoglobin. Nature 272, 506–510.

Eakin, C.M., Attenello, F.J., Morgan, C.J., and Miranker, A.D. (2004). Oligomeric assembly of native-like precursors precedes amyloid formation by β-2 microglobulin. Biochemistry 43, 7808–7815.

Elam, J.S., Taylor, A.B., Strange, R., Antonyuk, S., Doucette, P.A., Rodriguez, J.A., Hasnain, S.S., Hayward, L.J., Valentine, J.S., Yeates, T.O., and Hart, P.J. (2003). Amyloid-like filaments and water-filled nanotubes formed by SOD1 mutant proteins linked to familial ALS. Nat. Struct. Biol. 10, 461–467.

Engh, R., Lobermann, H., Schneider, M., Wiegand, G., Huber, R., and Laurell, C.B. (1989). The S variant of human α 1-antitrypsin, structure and implications for function and metabolism. Protein Eng. 2, 407–415.

Esposito, L., and Daggett, V. (2005). Insight into ribonuclease A domain swapping by molecular dynamics unfolding simulations. Biochemistry 44, 3358–3368.

Fandrich, M., Forge, V., Buder, K., Kittler, M., Dobson, C.M., and Diekmann, S. (2003). Myoglobin forms amyloid fibrils by association of unfolded polypeptide segments. Proc. Natl. Acad. Sci. USA 100, 15463–15468.

Gotte, G., and Libonati, M. (2004). Oligomerization of ribonuclease A: two novel three-dimensional domain-swapped tetramers. J. Biol. Chem. 279, 36670–36679.

Gotte, G., Vottariello, F., and Libonati, M. (2003). Thermal aggregation of ribonuclease A. A contribution to the understanding of the

role of 3D domain swapping in protein aggregation. J. Biol. Chem. *278*, 10763–10769.

Gotte, G., Laurents, D.V., and Libonati, M. (2006). Three-dimensional domain-swapped oligomers of ribonuclease A: identification of a fifth tetramer, pentamers and hexamers, and detection of trace heptameric, octameric and nonameric species. Biochim. Biophys. Acta *1764*, 44–54.

Green, S.M., Gittis, A.G., Meeker, A.K., and Lattman, E.E. (1995). One-step evolution of a dimer from a monomeric protein. Nat. Struct. Biol. *2*, 746–751.

Holmes, K.C., Popp, D., Gebhard, W., and Kabsch, W. (1990). Atomic model of the actin filament. Nature *347*, 44–49.

Huntington, J.A., Pannu, N.S., Hazes, B., Read, R.J., Lomas, D.A., and Carrell, R.W. (1999). A 2.6 Å structure of a serpin polymer and implications for conformational disease. J. Mol. Biol. *293*, 449–455.

Janowski, R., Kozak, M., Jankowska, E., Grzonka, Z., Grubb, A., Abrahamson, M., and Jaskolski, M. (2001). Human cystatin C, an amyloidogenic protein, dimerizes through three-dimensional domain swapping. Nat. Struct. Biol. *8*, 316–320.

Janowski, R., Abrahamson, M., Grubb, A., and Jaskolski, M. (2004). Domain swapping in N-truncated human cystatin C. J. Mol. Biol. *341*, 151–160.

Janowski, R., Kozak, M., Abrahamson, M., Grubb, A., and Jaskolski, M. (2005). 3D domain-swapped human cystatin C with amyloidlike intermolecular β-sheets. Proteins *61*, 570–578.

Jaskolski, M. (2001). 3D domain swapping, protein oligomerization, and amyloid formation. Acta Biochim. Pol. *48*, 807–827.

Jencks, W.P. (1981). On the attribution and additivity of binding energies. Proc. Natl. Acad. Sci. USA *78*, 4046–4050.

Kallberg, Y., Gustafsson, M., Persson, B., Thyberg, J., and Johansson, J. (2001). Prediction of amyloid fibril-forming proteins. J. Biol. Chem. *276*, 12945–12950.

Kaplan, B., Vidal, R., Kumar, A., Ghiso, J., Frangione, B., and Gallo, G. (1997). Amino-terminal identity of co-existent amyloid and non-amyloid immunoglobulin κ light chain deposits. A human disease to study alterations of protein conformation. Clin. Exp. Immunol. *110*, 472–478.

Knaus, K.J., Morillas, M., Swietnicki, W., Malone, M., Surewicz, W.K., and Yee, V.C. (2001). Crystal structure of the human prion protein reveals a mechanism for oligomerization. Nat. Struct. Biol. *8*, 770–774.

Lawson, C.L., Benoff, B., Berger, T., Berman, H.M., and Carey, J. (2004). *E. coli* trp repressor forms a domain-swapped array in aqueous alcohol. Structure (Camb) *12*, 1099–1108.

Lee, S., and Eisenberg, D. (2003). Seeded conversion of recombinant prion protein to a disulfide-bonded oligomer by a reduction-oxidation process. Nat. Struct. Biol. *10*, 725–730.

Libonati, M., and Gotte, G. (2004). Oligomerization of bovine ribonuclease A: structural and functional features of its multimers. Biochem. J. *380*, 311–327.

Liu, Y., and Eisenberg, D. (2002). 3D domain swapping: as domains continue to swap. Protein Sci. *11*, 1285–1299.

Liu, Y., Hart, P.J., Schlunegger, M.P., and Eisenberg, D. (1998). The crystal structure of a 3D domain-swapped dimer of RNase A at a 2.1-Å resolution. Proc. Natl. Acad. Sci. USA *95*, 3437–3442.

Liu, Y., Gotte, G., Libonati, M., and Eisenberg, D. (2001). A domain-swapped RNase A dimer with implications for amyloid formation. Nat. Struct. Biol. *8*, 211–214.

Liu, Y., Gotte, G., Libonati, M., and Eisenberg, D. (2002). Structures of the two 3D domain-swapped RNase A trimers. Protein Sci. *11*, 371–380.

Loebermann, H., Tokuoka, R., Deisenhofer, J., and Huber, R. (1984). Human α 1-proteinase inhibitor. Crystal structure analysis of two crystal modifications, molecular model and preliminary analysis of the implications for function. J. Mol. Biol. *177*, 531–557.

Lomas, D.A., and Carrell, R.W. (2002). Serpinopathies and the conformational dementias. Nat. Rev. Genet. *3*, 759–768.

Louis, J.M., Byeon, I.J., Baxa, U., and Gronenborn, A.M. (2005). The GB1 amyloid fibril: recruitment of the peripheral β-strands of the domain swapped dimer into the polymeric interface. J. Mol. Biol. *348*, 687–698.

Makin, O.S., Atkins, E., Sikorski, P., Johansson, J., and Serpell, L.C. (2005). Molecular basis for amyloid fibril formation and stability. Proc. Natl. Acad. Sci. USA *102*, 315–320.

Mammen, M., Choi, S.-K., and Whitesides, G.M. (1998). Polyvalent interactions in biological systems: implications for design and use of multivalent ligands and inhibitors. Angew. Chem. Int. Ed. Engl. *37*, 2754–2794.

Mast, A.E., Enghild, J.J., and Salvesen, G. (1992). Conformation of the reactive site loop of alpha 1-proteinase inhibitor probed by limited proteolysis. Biochemistry *31*, 2720–2728.

Murray, A.J., Head, J.G., Barker, J.J., and Brady, R.L. (1998). Engineering an intertwined form of CD2 for stability and assembly. Nat. Struct. Biol. *5*, 778–782.

Nelson, R., Sawaya, M.R., Balbirnie, M., Madsen, A.O., Riekel, C., Grothe, R., and Eisenberg, D. (2005). Structure of the amyloid spine. Nature *435*, 773–778.

Nilsson, M., Wang, X., Rodziewicz-Motowidlo, S., Janowski, R., Lindstrom, V., Onnerfjord, P., Westermark, G., Grzonka, Z., Jaskolski, M., and Grubb, A. (2004). Prevention of domain swapping inhibits dimerization and amyloid fibril formation of cystatin C: use of engineered disulfide bridges, antibodies, and carboxymethylpapain to stabilize the monomeric form of cystatin C. J. Biol. Chem. *279*, 24236–24245.

Ogihara, N.L., Ghirlanda, G., Bryson, J.W., Gingery, M., DeGrado, W.F., and Eisenberg, D. (2001). Design of three-dimensional domain-swapped dimers and fibrous oligomers. Proc. Natl. Acad. Sci. USA *98*, 1404–1409.

Pepys, M.B. (2006). Amyloidosis. Annu. Rev. Med. *57*, 223–241.

Ponstingl, H., Henrick, K., and Thornton, J.M. (2000). Discriminating between homodimeric and monomeric proteins in the crystalline state. Proteins *41*, 47–57.

Prusiner, S.B. (1998). Prions. Proc. Natl. Acad. Sci. USA *95*, 13363–13383.

Rousseau, F., Schymkowitz, J.W., and Itzhaki, L.S. (2003). The unfolding story of three-dimensional domain swapping. Structure *11*, 243–251.

Rousseau, F., Schymkowitz, J.W., Wilkinson, H.R., and Itzhaki, L.S. (2004). Intermediates control domain swapping during folding of p13suc1. J. Biol. Chem. *279*, 8368–8377.

Sambashivan, S., Liu, Y., Sawaya, M.R., Gingery, M., and Eisenberg, D. (2005). Amyloid-like fibrils of ribonuclease A with 3D domain-swapped, native-like structure. Nature *437*, 266–269.

Sanders, A., Jeremy Craven, C., Higgins, L.D., Giannini, S., Conroy, M.J., Hounslow, A.M., Waltho, J.P., and Staniforth, R.A. (2004). Cystatin forms a tetramer through structural rearrangement of domain-swapped dimers prior to amyloidogenesis. J. Mol. Biol. *336*, 165–178.

Sanner, M.F., Olson, A.J., and Spehner, J.C. (1996). Reduced surface: an efficient way to compute molecular surfaces. Biopolymers *38*, 305–320.

Sawaya, M.R., Guo, S., Tabor, S., Richardson, C.C., and Ellenberger, T. (1999). Crystal structure of the helicase domain from the replicative helicase-primase of bacteriophage T7. Cell *99*, 167–177.

Schevitz, R.W., Otwinowski, Z., Joachimiak, A., Lawson, C.L., and Sigler, P.B. (1985). The three-dimensional structure of trp repressor. Nature *317*, 782–786.

Serag, A.A., Altenbach, C., Gingery, M., Hubbell, W.L., and Yeates, T.O. (2002). Arrangement of subunits and ordering of β-strands in an amyloid sheet. Nat. Struct. Biol. *9*, 734–739.

Shuker, S.B., Hajduk, P.J., Meadows, R.P., and Fesik, S.W. (1996). Discovering high-affinity ligands for proteins: SAR by NMR. Science *274*, 1531–1534.

Singleton, M.R., Sawaya, M.R., Ellenberger, T., and Wigley, D.B. (2000). Crystal structure of T7 gene 4 ring helicase indicates a mechanism for sequential hydrolysis of nucleotides. Cell *101*, 589–600.

Sipe, J.D., and Cohen, A.S. (2000). Review: history of the amyloid fibril. J. Struct. Biol. *130*, 88–98.

Spinelli, S., Desmyter, A., Frenken, L., Verrips, T., Tegoni, M., and Cambillau, C. (2004). Domain swapping of a llama VHH domain builds a crystal-wide β-sheet structure. FEBS Lett. *564*, 35–40.

Stokes, M.B., Jagirdar, J., Burchstin, O., Kornacki, S., Kumar, A., and Gallo, G. (1997). Nodular pulmonary immunoglobulin light chain deposits with coexistent amyloid and nonamyloid features in an HIV-infected patient. Mod. Pathol. *10*, 1059–1065.

Story, R.M., Weber, I.T., and Steitz, T.A. (1992). The structure of the *E. coli* recA protein monomer and polymer. Nature *355*, 318–325.

Strop, P., Smith, K.S., Iverson, T.M., Ferry, J.G., and Rees, D.C. (2001). Crystal structure of the "cab"-type β class carbonic anhydrase from the archaeon *Methanobacterium thermoautotrophicum*. J. Biol. Chem. *276*, 10299–10305.

Su, X.D., Gastinel, L.N., Vaughn, D.E., Faye, I., Poon, P., and Bjorkman, P.J. (1998). Crystal structure of hemolin: a horseshoe shape with implications for homophilic adhesion. Science *281*, 991–995.

Suarez Covarrubias, A., Larsson, A.M., Hogbom, M., Lindberg, J., Bergfors, T., Bjorkelid, C., Mowbray, S.L., Unge, T., and Jones, T.A. (2005). Structure and function of carbonic anhydrases from *Mycobacterium tuberculosis*. J. Biol. Chem. *280*, 18782–18789.

Sunde, M., Serpell, L.C., Bartlam, M., Fraser, P.E., Pepys, M.B., and Blake, C.C. (1997). Common core structure of amyloid fibrils by synchrotron X-ray diffraction. J. Mol. Biol. *273*, 729–739.

Taylor, P., Dornan, J., Carrello, A., Minchin, R.F., Ratajczak, T., and Walkinshaw, M.D. (2001). Two structures of cyclophilin 40: folding and fidelity in the TPR domains. Structure (Camb) *9*, 431–438.

Thirumalai, D., Klimov, D.K., and Dima, R.I. (2003). Emerging ideas on the molecular basis of protein and peptide aggregation. Curr. Opin. Struct. Biol. *13*, 146–159.

Westermark, P., Benson, M.D., Buxbaum, J.N., Cohen, A.S., Frangione, B., Ikeda, S., Masters, C.L., Merlini, G., Saraiva, M.J., and Sipe, J.D. (2005). Amyloid: toward terminology clarification. Report from the Nomenclature Committee of the International Society of Amyloidosis. Amyloid *12*, 1–4.

Wishner, B.C., Ward, K.B., Lattman, E.E., and Love, W.E. (1975). Crystal structure of sickle-cell deoxyhemoglobin at 5 Å resolution. J. Mol. Biol. *98*, 179–194.

Xing, X., and Bell, C.E. (2004). Crystal structures of *Escherichia coli* RecA in a compressed helical filament. J. Mol. Biol. *342*, 1471–1485.

Yang, F., Bewley, C.A., Louis, J.M., Gustafson, K.R., Boyd, M.R., Gronenborn, A.M., Clore, G.M., and Wlodawer, A. (1999). Crystal structure of cyanovirin-N, a potent HIV-inactivating protein, shows unexpected domain swapping. J. Mol. Biol. *288*, 403–412.

Yu, X., and Egelman, E.H. (1997). The RecA hexamer is a structural homologue of ring helicases. Nat. Struct. Biol. *4*, 101–104.

Zahn, R., Liu, A., Luhrs, T., Riek, R., von Schroetter, C., Lopez Garcia, F., Billeter, M., Calzolai, L., Wider, G., and Wuthrich, K. (2000). NMR solution structure of the human prion protein. Proc. Natl. Acad. Sci. USA *97*, 145–150.